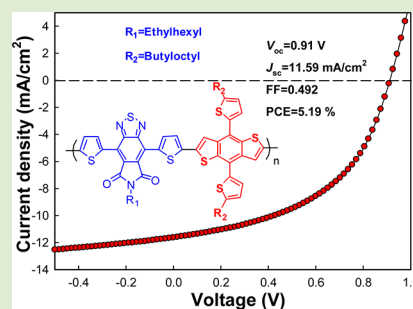


## Low Band Gap Polymers Incorporating a Dicarboxylic Imide-Derived Acceptor Moiety for Efficient Polymer Solar Cells

Lixin Wang,<sup>†,‡</sup> Dongdong Cai,<sup>†</sup> Qingdong Zheng,<sup>\*,†</sup> Changquan Tang,<sup>†</sup> Shan-Ci Chen,<sup>†</sup> and Zhigang Yin<sup>†</sup><sup>†</sup>State Key Laboratory of Structural Chemistry, Fujian Institute of Research on the Structure of Matter, Chinese Academy of Sciences, 155 Yangqiao West Road, Fuzhou, Fujian 350002, P. R. China<sup>‡</sup>Graduate University of Chinese Academy of Sciences, Beijing 100049, P. R. China

## Supporting Information

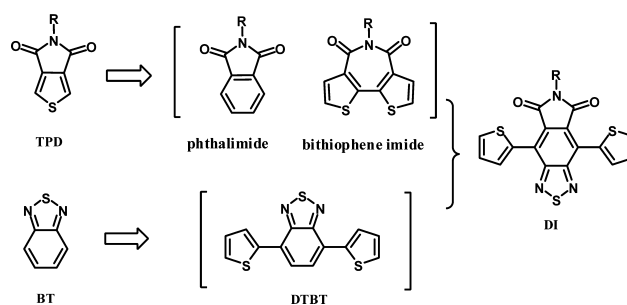
**ABSTRACT:** Two novel copolymers incorporating *N*-alkyl-4,7-di(thien-2-yl)-2,1,3-benzothiadiazole-5,6-dicarboxylic imide (DI) and benzo[1,2-*b*:4,5-*b'*]dithiophene (BDT) units have been designed, synthesized, and characterized. By the incorporation of the DI unit, both polymers show a bathochromically shifted absorption with a deep lying highest occupied molecular orbital (HOMO) energy level. The polymer based on thienyl group substituted BDT exhibits an intense absorption in the longer-wavelength region, a deeper lying HOMO energy level, and a higher carrier mobility, all of which contribute to the resulting polymer solar cells with a higher power conversion efficiency (PCE) of 5.19% and an increased  $V_{oc}$  of 0.91 V.



Polymer solar cells (PSCs) have arrested great attention from both the academic and industrial community because they can be fabricated as lightweight, large-area, and flexible devices by low-cost solution processing methods.<sup>1</sup> Bulk heterojunction (BHJ) PSCs, in which a phase-separated blend of donor materials and acceptor materials is sandwiched between an anode and a cathode, are promising in realizing high power conversion efficiency (PCE) devices.<sup>2</sup> To date, PCEs over 9% for a single junction cell have been achieved.<sup>3</sup> For a PSC, polymers in the active layer play an important role in determining the number of harvested photons and the resulting PCE. Now it is well recognized that the donor–acceptor (D–A) copolymer strategy is effective in constructing efficient low band gap polymers because it will not only extend the absorption bands but also provide deep-lying HOMO energy levels of the target polymers.<sup>3,4</sup> In the past 5 years, a large number of donor units for D–A copolymers have been reported, which include fluorene, bithiophene, carbazole, cyclopentadithiophene, indenofluorene, benzodithiophene etc.<sup>3a,5</sup> However, efficient acceptor units are relatively rare. Thus, there is an urgent need to research novel acceptor units for D–A copolymers.

Both benzothiadiazole (BT) and dithiophene-benzothiadiazole (DTBT) are excellent acceptor units for highly efficient low band gap polymers, and PSCs based on these polymers exhibited PCEs as high as 7.2%.<sup>6</sup> Other frequently used acceptor units are mainly based on a strong electron-deficient dicarboxylic imide, such as thieno[3,4-*c*]pyrrole-4,6-dione (TPD), phthalimide, and 2,2'-bithiophene-3,3'-dicarboxylic imide (Scheme 1).<sup>7</sup> D–A copolymers based on these dicarboxylic imide-derived acceptor units have been successfully used for fabricating efficient PSCs with PCEs in the range of

## Scheme 1. Chemical Structures of Dicarboxylic Imide-Derived Acceptors and Benzothiadiazole-Derived Acceptors



4.2–7.4%.<sup>7</sup> Besides, D–A copolymers containing dicarboxylic imide units (e.g., TPD) usually have deep-lying HOMO energy levels, which led to large open circuit voltages of the fabricated devices.<sup>7</sup> Therefore, if a dicarboxylic imide is integrated into the BT group, a stronger acceptor unit can be obtained, which may have combined advantages from both the BT and the dicarboxylic imide group. For example, different soluble groups can be introduced into the dicarboxylic imide building block for a better solubility of the acceptor unit. Furthermore, its stronger electron-deficient nature will lead to low band gap copolymers with a deeper lying HOMO level. As for the donor units, benzo[1,2-*b*:4,5-*b'*]dithiophene (BDT) is one of the best building blocks for efficient low band gap copolymers.<sup>8–10</sup> By now, BDT-based copolymers have been used to make PSCs

Received: April 14, 2013

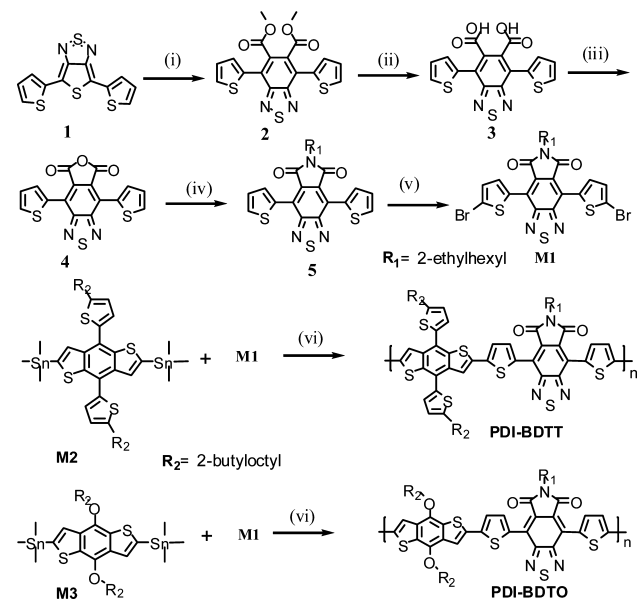
Accepted: June 19, 2013

Published: June 21, 2013

with a PCE up to 9.2%.<sup>3</sup> In this context, an electron-deficient acceptor (DI in Scheme 1) with a combined chemical structure of the DTBT and the dicarboxylic imide is synthesized. Two novel D–A copolymers based on DI and BDT units are designed, prepared, and used as donor materials for PSCs for the first time.

The synthesis of the DI-based monomer (**M1**) is depicted in Scheme 2. Compound **2** was prepared in 83% yield by reacting

**Scheme 2.** (i) Dimethyl Acetylenedicarboxylate, Xylene; (ii) NaOH, EtOH; (iii) Ac<sub>2</sub>O, Xylene; (iv) 2-Ethyl-1-hexylamine, AcOH, then Ac<sub>2</sub>O; (v) NBS, THF; (vi) Pd(PPh<sub>3</sub>)<sub>4</sub>, Toluene, DMF



compound **1** with dimethyl acetylenedicarboxylate in xylene at 100 °C. Then the hydrolysis of compound **2** afforded a dicarboxylic acid derivative **3**, which was then converted to compound **4** in 64% yield in the presence of acetic anhydride. An alkylation reaction of compound **4** gave the key intermediate **5**, which was brominated by NBS to give the monomer **M1**. During the preparation of this manuscript, we noticed that two different methods had been reported for the DI synthesis. However, neither of them was synthesized for constructing donor–acceptor copolymers in organic solar cells.<sup>11</sup> Monomers **M2** and **M3** were obtained according to the published procedures.<sup>5b</sup> Two long alkyl chains were introduced into the BDT core to improve the solubility of the target polymers (Scheme 2). Finally, a Stille coupling reaction between **M1** and **M2** (or **M3**) using Pd(PPh<sub>3</sub>)<sub>4</sub> as a catalyst afforded the target polymer **PDI-BDTT** (or **PDI-BDTO**). Both polymers have good solubility in common solvents such as chloroform, chlorobenzene, etc. The number-average molecular weights (*M<sub>n</sub>*) determined by gel permeation chromatography (GPC) using polystyrene as standard and THF as eluent were 29 and 44 kDa, with polydispersity indices (PDIs) of 4.8 and 3.2, for **PDI-BDTT** and **PDI-BDTO**, respectively.

The absorption spectra for the target polymers in dilute chlorobenzene solution and in thin film are shown in Figure 1. The absorption maxima and optical band gaps are summarized in Table 1. Each polymer has one absorption band at the shorter wavelength region which is due to localized  $\pi$ – $\pi^*$

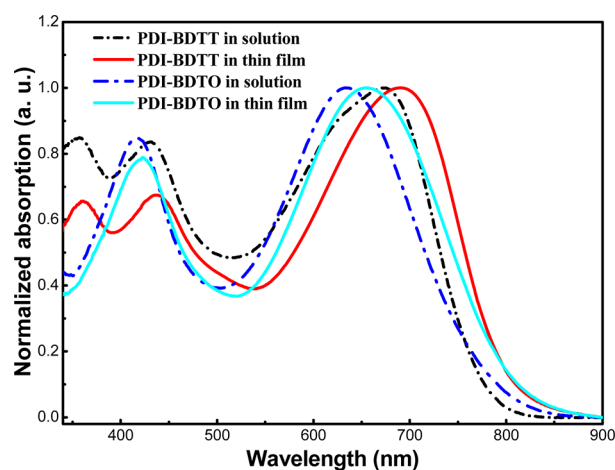


**Figure 1.** Absorption spectra of PDI-BDTT and PDI-BDTO in solution (chlorobenzene,  $1 \times 10^{-5}$  M) and in thin film.

transitions and one absorption band at the longer wavelength region which is due to intramolecular charge transfer. In solution, PDI-BDTT exhibits a red-shifted absorption maximum of 670 nm compared to PDI-BDTO ( $\lambda_{\text{max}} = 632$  nm), which can be attributed to the extended  $\pi$ -conjugation length by incorporating the two thienyl groups in PDI-BDTT. Both polymers in thin film show bathochromic absorption bands in comparison with their corresponding polymer solutions (692 vs 670 nm for PDI-BDTT and 654 vs 632 nm for PDI-BDTO), indicating a strong intermolecular stacking for the polymers in the solid state. The optical band gaps deduced from the absorption edges of thin film spectra were estimated to be 1.55 and 1.54 eV for PDI-BDTT and PDI-BDTO, respectively. Cyclic voltammetry measurements were performed to determine the HOMO and LUMO energy levels of these two polymers (see Figure S1, Supporting Information), and the electrochemical data are listed in Table 1. On the basis of the onset oxidation potentials, the HOMO levels of PDI-BDTT and PDI-BDTO were estimated to be  $-5.51$  and  $-5.44$  eV, respectively, and based on the onset reduction potentials, their LUMO levels were estimated to be  $-3.76$  and  $-3.74$  eV, respectively. The electrochemical band gaps for PDI-BDTT and PDI-BDTO were calculated to be 1.75 and 1.70 eV, respectively. On the basis of the optical and electrochemical data of the two copolymers, one may find that the introduction of two substituted thienyl groups leads to a copolymer with a red-shifted absorption band as well as a deeper-lying HOMO level, which is beneficial to a higher  $V_{\text{oc}}$  and  $J_{\text{sc}}$  of the fabricated PSCs.

The photovoltaic properties of both polymers were investigated with a conventional device configuration using PEDOT:PSS as an interlayer. The current–voltage characteristics of the optimized devices are shown in Figure 2, and the device parameters are summarized in Table 1. The solar cell based on PDI-BDTT:PC<sub>71</sub>BM exhibited a  $V_{\text{oc}}$  of 0.91 V, a  $J_{\text{sc}}$  of 11.59 mA/cm<sup>2</sup>, a fill factor (FF) of 49.2%, and a PCE of 5.19%, while the PDI-BDTO:PC<sub>71</sub>BM-based device only showed a  $V_{\text{oc}}$  of 0.80 V, a  $J_{\text{sc}}$  of 5.53 mA/cm<sup>2</sup>, a FF of 47.1%, and a PCE of 2.10% under the same device fabrication conditions. Obviously, the PDI-BDTT:PC<sub>71</sub>BM-based device outperforms the device based on PDI-BDTO:PC<sub>71</sub>BM. Furthermore, the blend ratio and the additive concentration also affected the device performance of these two polymers (Table S1–S2, Supporting Information). Compared to the analogous polymer PBDTTBT

**Table 1. Summary of Intrinsic Properties and Photovoltaic Characteristics (under AM 1.5G, 100 mW/cm<sup>2</sup>) for the Polymers**

| polymer  | $M_n^a$  | $\lambda_{\max}$ (nm) |      | $E_{g,opt}^b$ | HOMO <sup>c</sup> | LUMO <sup>c</sup> | $E_{g,elec.}$ | $\mu_{hole}$  | $J_{sc}$              | $V_{oc}$ | FF   | PCE  |
|----------|----------|-----------------------|------|---------------|-------------------|-------------------|---------------|---|-----------------------|----------|------|------|
|          | (kg/mol) | solution              | film | (eV)          | (eV)              | (eV)              | (eV)          | (cm <sup>2</sup> V <sup>-1</sup> s <sup>-1</sup> ) <sup>d</sup> | (mA/cm <sup>2</sup> ) | (V)      | (%)  | (%)  |
| PDI-BDTT | 29       | 670                   | 692  | 1.55          | -5.51             | -3.76             | 1.75          | $1.78 \times 10^{-5}$   | 11.59                 | 0.91     | 49.2 | 5.19 |
| PDI-BDTO | 44       | 632                   | 654  | 1.54          | -5.44             | -3.74             | 1.70          | $6.8 \times 10^{-7}$  | 5.53                  | 0.80     | 47.1 | 2.10 |

<sup>a</sup>The number-average molecular weights measured by GPC. <sup>b</sup>From the edge of absorption spectra in thin film. <sup>c</sup>From the onset of CV in thin film. <sup>d</sup>By a SCLC method.

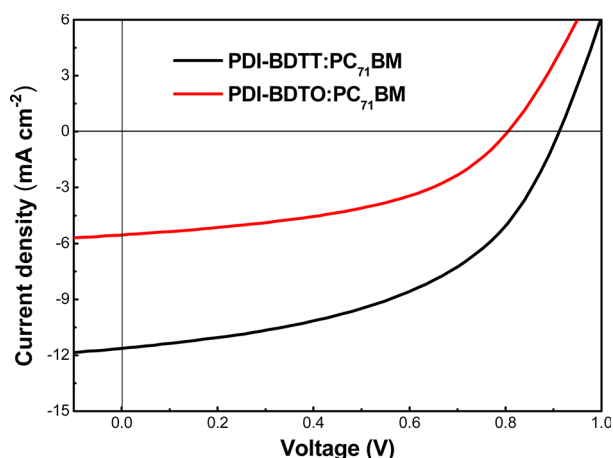


**Figure 2.**  $J$ - $V$  characteristics of PSCs based on PDI-BDTT:PC<sub>71</sub>BM and PDI-BDTO:PC<sub>71</sub>BM under AM 1.5G illumination (100 mW cm<sup>-2</sup>).

based on DTBT and thienyl-substituted BDT, PDI-BDTT possesses red-shifted absorption (i.e., film absorption peak: 692 vs 596 nm). Subsequently, the device based on PDI-BDTT exhibits a higher  $J_{sc}$  of 11.59 mA/cm<sup>2</sup> with a high  $V_{oc}$  of 0.91 V, in comparison with the device based on PBDTTBT ( $J_{sc}$  = 10.70 mA/cm<sup>2</sup>,  $V_{oc}$  of 0.92 V). The results demonstrate that PDI-BDTT would be a better candidate as a longer-wavelength absorbing material for efficient tandem solar cells.<sup>8b</sup>

The external quantum efficiency (EQE) curves of the PSCs based on PDI-BDTT:PC<sub>71</sub>BM or PDI-BDTO:PC<sub>71</sub>BM were measured under illumination of monochromatic light (Figure S2, Supporting Information). From the EQE spectra, one may find that both devices have a broad photon response range from ~300 to ~790 nm, which is in agreement with the corresponding absorption spectrum of the blended thin films (Figure S3, Supporting Information). However, the EQE values for the PDI-BDTT-based device are all higher than those for the PDI-BDTO-based device, which agree with the higher  $J_{sc}$  observed for the PDI-BDTT-based device. To get more insight into the better performance for PDI-BDTT-based devices compared with that for PDI-BDTO-based devices, we measured the hole mobilities of both polymers (blended with PC<sub>71</sub>BM) using a space charge limited current (SCLC) method (Figure S4, Supporting Information), and the results are listed in Table 1. It was found that the hole mobility of PDI-BDTT was  $1.78 \times 10^{-5}$  cm<sup>2</sup> V<sup>-1</sup> s<sup>-1</sup>, which is more than 1 order of magnitude higher than that of PDI-BDTO ( $6.8 \times 10^{-7}$  cm<sup>2</sup> V<sup>-1</sup> s<sup>-1</sup>). In comparison with PDI-BDTO, the polymer backbone of PDI-BDTT has two additional thienyl groups flanked on the BDT unit, which leads to a better intramolecular stacking induced by the more extended  $\pi$ -conjugation.<sup>8a</sup> Therefore, a greatly increased hole mobility was found for PDI-BDTT, which is the main reason for the increased  $J_{sc}$  value of the PSC device based on PDI-BDTT. The morphology of the blended

films fabricated under the same conditions as those for the optimized devices was evaluated by atomic force microscopy (AFM). As shown in Figure 3, the blended film based on PDI-

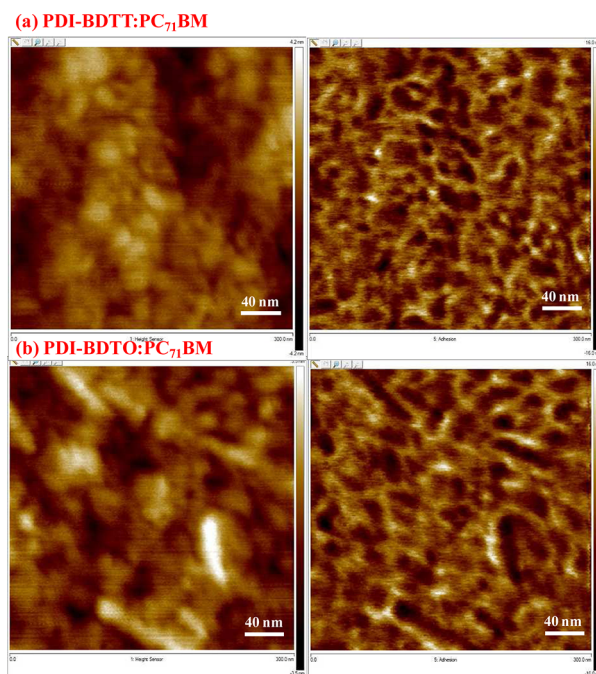


**Figure 3.** AFM topography images (left,  $1 \times 1 \mu\text{m}^2$ ) and phase images (right,  $1 \times 1 \mu\text{m}^2$ ) of PDI-BDTT:PC<sub>71</sub>BM (a) and PDI-BDTO:PC<sub>71</sub>BM (b) films.

BDTT:PC<sub>71</sub>BM (1:2, w/w) has a smooth surface (roughness = 0.89 nm) and continuous phase separation domains of ~10–20 nm, indicating its good nanosized morphological property for the efficient charge separation and transport. Similarly, the blended film based on PDI-BDTO:PC<sub>71</sub>BM (1:2, w/w) also has an obvious phase separation feature.

In conclusion, two D–A copolymers using DI as the acceptor unit, PDI-BDTT and PDI-BDTO, were developed for PSCs for the first time. By the incorporation of the DI unit, PDI-BDTT showed a pronounced bathochromically shifted absorption with a deep lying HOMO energy level. With a relatively high  $V_{oc}$  of 0.91 V, a fairly high  $J_{sc}$  of 11.59 mA/cm<sup>2</sup>, and a FF of 0.49, the PSC device based on PDI-BDTT achieved a PCE of 5.19%. The polymer based on thienyl group substituted BDT exhibited red-shifted absorption, a deeper HOMO level, a higher mobility, and improved photovoltaic properties compared to that with the alkoxy-substituted analogue. With its intense absorption in the longer-wavelength region, a deep lying HOMO energy level, and good photovoltaic performance, PDI-BDTT shows good potential as a long-wavelength absorbing material in tandem solar cells with a high  $V_{oc}$ . Further studies are currently ongoing to prepare PDI-BDTT with an optimized



molecular weight and to fabricate the corresponding tandem solar cells.

## ■ ASSOCIATED CONTENT

### ■ Supporting Information

Experimental details, synthesis, and characterization of monomers and polymers, photovoltaic parameters of PSCs fabricated under different conditions, solar cell fabrication procedure, electrochemical cyclic voltammetry, external quantum efficiency (EQE) curves, absorption spectra of blended films, and hole mobility measurement of the polymers. This material is available free of charge via the Internet at <http://pubs.acs.org>.

## ■ AUTHOR INFORMATION

### Corresponding Author

\*Tel. +86-591-83721625. Fax: +86-591-83721625. E-mail: [qingdongzheng@fjirsm.ac.cn](mailto:qingdongzheng@fjirsm.ac.cn).

### Notes

The authors declare no competing financial interest.

## ■ ACKNOWLEDGMENTS

This work was in part supported by National Science Foundation of China (51173186) and in part by the 100 Talents Programme of The Chinese Academy of Sciences. We thank Dr. Hao Sun and Fei Long from Bruker China and Danmei Pan from our institute for their help in AFM.

## ■ REFERENCES

- (1) (a) Arias, A. C.; MacKenzie, J. D.; McCulloch, I.; Rivnay, J.; Salleo, A. *Chem. Rev.* **2010**, *110*, 3–24. (b) Chen, H. Y.; Hou, J. H.; Zhang, S. Q.; Liang, Y. Y.; Yang, G. W.; Yang, Y.; Yu, L. P.; Wu, Y.; Li, G. *Nat. Photon.* **2009**, *3*, 649–653. (c) Li, G.; Zhu, R.; Yang, Y. *Nat. Photon.* **2012**, *6*, 153–161. (d) Yang, D.; Zhou, L. Y.; Chen, L. C.; Zhao, B.; Zhang, J.; Li, C. *Chem. Commun.* **2012**, *48*, 8078–8080.
- (2) Yu, G.; Gao, J.; Hummelen, J. C.; Wudl, F.; Heeger, A. J. *Science* **1995**, *270*, 1789–1791.
- (3) (a) Cheng, Y. J.; Yang, S. H.; Hsu, C. S. *Chem. Rev.* **2009**, *109*, 5868–5923. (b) Zhou, H. X.; Yang, L. Q.; You, W. *Macromolecules* **2012**, *45*, 607–632. (c) He, Z. C.; Zhong, C. M.; Su, S. J.; M., X.; Wu, H. B.; Cao, Y. *Nat. Photon.* **2012**, *6*, 591–595.
- (4) (a) Yue, W.; Zhao, Y.; Shao, S. Y.; Tian, H. K.; Xie, Z. Y.; Geng, Y. H.; Wang, F. S. *J. Mater. Chem.* **2009**, *19*, 2199–2206. (b) Shi, Q. Q.; Fan, H. J.; Liu, Y.; Chen, J. M.; Ma, L. C.; Hu, W. P.; Shuai, Z. G.; Li, Y. F.; Zhan, X. W. *Macromolecules* **2011**, *44*, 4230–4240.
- (5) (a) Park, S. H.; Roy, A.; Beaupre, S.; Cho, S.; Coates, N.; Moon, J. S.; Moses, D.; Leclerc, M.; Lee, K.; Heeger, A. J. *Nat. Photon.* **2009**, *3*, 297–302. (b) Liang, Y. Y.; Wu, Y.; Feng, D. Q.; Tsai, S. T.; Son, H. J.; Li, G.; Yu, L. P. *J. Am. Chem. Soc.* **2009**, *131*, 56–57. (c) Boudreault, P.-L. T.; Najari, A.; Leclerc, M. *Chem. Mater.* **2011**, *23*, 456–469.
- (6) (a) Cheng, Y. J.; Chen, C. H.; Lin, Y. S.; Chang, C. Y.; Hsu, C. S. *Chem. Mater.* **2011**, *23*, 5068–5075. (b) Zhou, H. X.; Yang, L. Q.; Stuart, A. C.; Price, S. C.; Liu, S. B.; You, W. *Angew. Chem., Int. Ed.* **2011**, *50*, 2995–2998. (c) Zheng, Q. D.; Jung, B. J.; Sun, J.; Katz, H. E. *J. Am. Chem. Soc.* **2010**, *132*, 5394–5404. (d) Wang, M.; Li, C. H.; Lv, A. F.; Wang, Z. H.; Bo, Z. S. *Macromolecules* **2012**, *45*, 3017–3022.
- (7) (a) Amb, C. M.; Chen, S.; Graham, K. R.; Subbiah, J.; Small, C. E.; So, F.; Reynolds, J. R. *J. Am. Chem. Soc.* **2011**, *133*, 10062–10065. (b) Chu, T. Y.; Lu, J. P.; Beaupré, S.; Zhang, Y. G.; Pouliot, J. R.; Wakim, S.; Zhou, J. Y.; Leclerc, M.; Li, Z.; Ding, J. F.; Tao, Y. *J. Am. Chem. Soc.* **2011**, *133*, 4250–4253. (c) Zhou, N.; Guo, X.; Ortiz, R. P.; Li, S.; Zhang, S.; Chang, R. P.; Facchetti, A.; Marks, T. J. *Adv. Mater.* **2012**, *24*, 2242–2248. (d) Zhang, G. B.; Fu, Y. Y.; Zhang, Q.; Xie, Z. Y. *Chem. Commun.* **2010**, *46*, 4997–4999. (e) Zhang, Y.; Hau, S. K.; Yip, H. L.; Sun, Y.; Acton, O.; Jen, A. K. Y. *Chem. Mater.* **2010**, *22*, 2696–2698. (f) Zhang, W.; Cao, J. M.; Liu, Y.; Xiao, Z.; Zhu, W. G.;

Zuo, Q. Q.; Ding, L. M. *Macromol. Rapid Commun.* **2012**, *33*, 1574–1579. (g) Xin, H.; Guo, X. G.; Ren, G. Q.; Watson, M. D.; Jenekhe, S. A. *Adv. Energy Mater.* **2012**, *2*, 575–582.

(8) (a) Huo, L. J.; Zhang, S. Q.; Guo, X.; Xu, F.; Li, Y. F.; Hou, J. H. *Angew. Chem., Int. Ed.* **2011**, *50*, 9697–9702. (b) Huo, L.; Hou, J.; Zhang, S.; Chen, H.-Y.; Yang, Y. *Angew. Chem., Int. Ed.* **2010**, *49*, 1500–1503.

(9) Liang, Y. Y.; Yu, L. P. *Acc. Chem. Res.* **2010**, *43*, 1227–1236.

(10) Wang, M.; Hu, X.; Liu, P.; Li, W.; Gong, X.; Huang, F.; Cao, Y. *J. Am. Chem. Soc.* **2011**, *133*, 9638–9641.

(11) (a) Li, H. R.; Koh, T. M.; Hagfeldt, A.; Gratzel, M.; Mhaisalkar, S. G.; Grimsdale, A. C. *Chem. Commun.* **2013**, *49*, 2409–2411. (b) Shao, J.; Chang, J.; Chi, C. *Org. Biomol. Chem.* **2012**, *10*, 7045–7052.